

# Hydrogen Transfer Pathways during Zeolite Catalyzed Methanol Conversion to Hydrocarbons

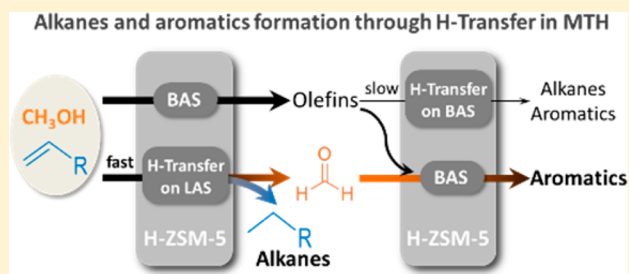
Sebastian Müller,<sup>†,§,||</sup> Yue Liu,<sup>†,§</sup> Felix M. Kirchberger,<sup>†</sup> Markus Tonigold,<sup>‡</sup> Maricruz Sanchez-Sanchez,<sup>\*,†</sup> and Johannes A. Lercher<sup>\*,†</sup>

<sup>†</sup>Department of Chemistry and Catalysis Research Center, Technische Universität München, Lichtenbergstr., 4, 85747 Garching, Germany

<sup>‡</sup>Clariant Produkte (Deutschland) GmbH, Waldheimer Str. 13, 83052 Bruckmühl, Germany

**S** Supporting Information

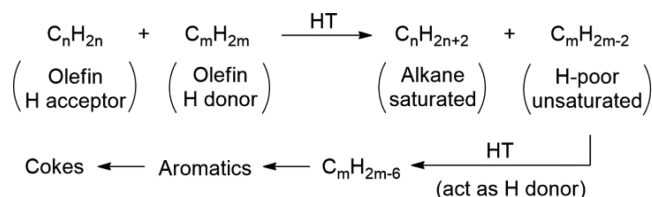
**ABSTRACT:** Hydrogen transfer is the major route in catalytic conversion of methanol to olefins (MTO) for the formation of nonolefinic byproducts, including alkanes and aromatics. Two separate, noninterlinked hydrogen transfer pathways have been identified. In the absence of methanol, hydrogen transfer occurs between olefins and naphthenes via protonation of the olefin and the transfer of the hydride to the carbenium ion. A hitherto unidentified hydride transfer pathway involving Lewis and Brønsted acid sites dominates as long as methanol is present in the reacting mixture, leading to aromatics and alkanes. Experiments with purely Lewis acidic ZSM-5 showed that methanol and propene react on Lewis acid sites to HCHO and propane. In turn, HCHO reacts with olefins stepwise to aromatic molecules on Brønsted acid sites. The aromatic molecules formed at Brønsted acid sites have a high tendency to convert to irreversibly adsorbed carbonaceous deposits and are responsible for the critical deactivation in the methanol to olefin process.



## 1. INTRODUCTION

The synthesis of olefins from methanol on zeolites and zeotype materials has been intensely studied<sup>1</sup> as an alternative route to generate light olefins.<sup>1–4</sup> In this solid acid catalyzed conversion C<sub>2–5</sub> olefins are formed from an equilibrium mixture of methanol and dimethyl ether. These olefins are methylated to higher olefins, which in turn are catalytically cracked again to lower olefins. Olefins, however, also react to alkanes and aromatics via hydrogen transfer (HT) and subsequently form coke (Scheme 1).<sup>2,4</sup> Thus, the qualitative and quantitative

**Scheme 1. Conventional Hydrogen Transfer between Olefins, Leading to Alkanes, Aromatics, and Coke**



understanding of hydrogen transfer reaction pathways, consisting of protonation and hydride transfer, is not only critical for the design of stable methanol-to-olefins (MTO) catalysts, but will also open new routes for carbon–carbon coupling in other organic synthesis routes.

Conventionally, the key step, the hydride transfer, is defined as a bimolecular reaction, in which a hydride is transferred between a hydride donor, frequently an alkane or alkene, and a hydride acceptor, frequently a surface alkoxide or a carbenium ion.<sup>2</sup> The rates and activation energies of hydride transfer reactions depend on the stability of the carbenium ion formed upon donation of the hydride.<sup>2,5–8</sup> The fact that under MTO conditions mainly olefins are formed led to the assumption that hydrogen transfer reactions on H-ZSM-5 take place mostly between two olefinic species on Brønsted acid sites (BAS)<sup>1,2,9</sup> via a mechanism shown in Scheme 2 for the reaction of propene and 1-butene.

Gaining insight into the mechanism and kinetics of hydrogen transfer on zeolites is challenging, because the reaction involves alkoxides, which also react via different pathways, including olefin addition or isomerization.<sup>2</sup> For the reaction explored here the problem has been partly circumvented by conducting studies at mild temperatures (~473 K).<sup>2</sup> Under such conditions, the presence of a hydride transfer agent such as adamantane,<sup>10</sup> for example, favors the formation of alkanes without simultaneous formation of arenes in acid-catalyzed cohomologation of alkanes and dimethyl ether on H-BEA.<sup>11</sup> The structures of the molecules involved appear to be of critical importance; cyclic dienes were, for example, more effective in

Received: September 13, 2016

Published: November 16, 2016

Scheme 2. Typical Hydrogen Transfer Pathway between Two Olefinic Species on BAS, Exemplified for Propene and 1-butene

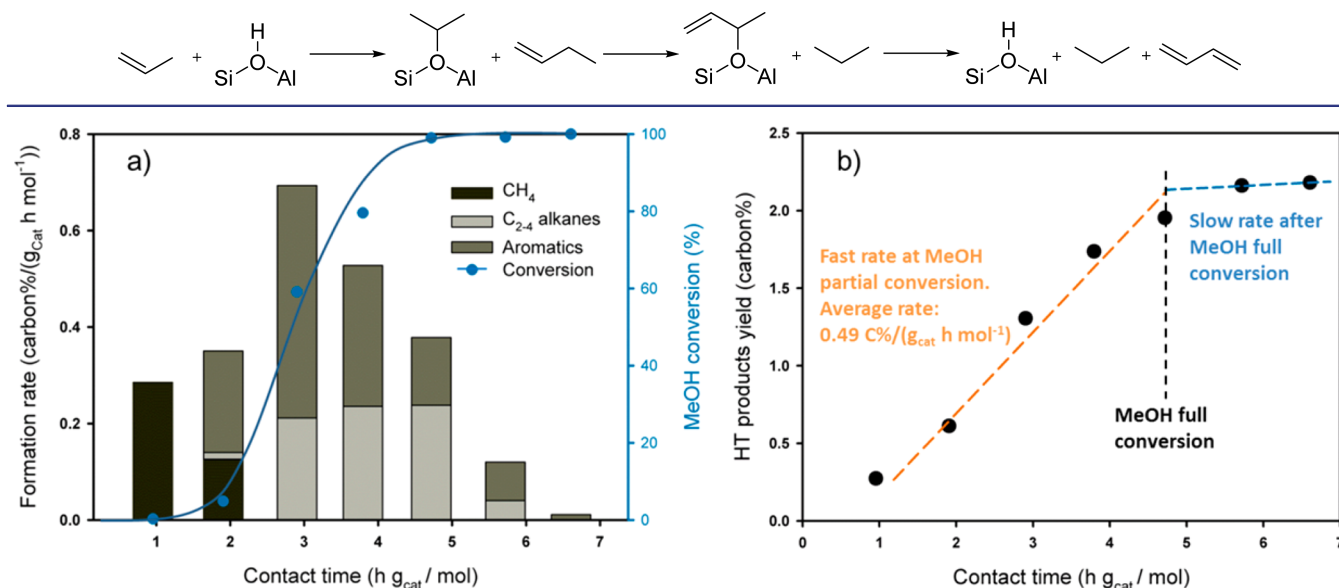


**Figure 1.** (a) Methanol conversion and formation rates of alkanes and aromatics as a function of contact time in reaction of methanol to olefins. (b) HT products (C<sub>1-4</sub> alkanes + aromatics) yield as a function of contact time (H-ZSM-5 (B 68, L 23) at  $p_{\text{MeOH}} = 178$  mbar and  $T = 723$  K). Rates are calculated as time site yield, the yield increase at a specific contact time:  $r = [d(\text{yield})]/[d(\text{contact time})]$ .

hydrogen transfer than the acyclic monoolefins during methanol homologation.<sup>12-16</sup>

Two possible routes to aromatics and alkanes from olefins must be considered. One route involves dehydrogenation of olefins to dienes and trienes that subsequently undergo cyclization to aromatic molecules.<sup>2</sup> On the other hand, higher olefins may cyclize and form aromatics by hydrogen transfer reactions after the cyclization. Both pathways are thought to link the olefin interconversions and the catalytic chemistry of aromatic molecules in the so-called dual-cycle model proposed for the methanol to hydrocarbons reaction.<sup>1,4,17,18</sup> In both cases, olefins act as hydrogen acceptors forming alkanes. As hydrogen transfer requires sterically demanding bimolecular transition states, reactions between higher olefins may be limited in medium pore zeolites such as H-ZSM-5 due to spatial constraints.<sup>19</sup>

Several studies addressed the interactions of BAS and Lewis acid sites (LAS) in the hydrogen transfer reactions of olefins.<sup>20-23</sup> Bortnovsky et al.,<sup>20</sup> for instance, observed the formation of bulky aromatics and alkanes in pentene cracking for catalysts with high concentrations of both strong BAS and LAS, suggesting that strong acid sites favor hydrogen transfer. Wichterlová et al.<sup>21</sup> reported the presence of LAS in zeolites to enhance both the strength of Brønsted acid sites and the rate of hydrogen transfer reactions. Sazama et al.<sup>23</sup> proposed LAS in H-ZSM-5 to favor oligomerization and hydrogen transfer reactions in MTH reactions, leading eventually to coke formation. Expanding from these examples, it is interesting to note that despite ample evidence of the positive impact of LAS on hydride transfer, little mechanistic evidence for a specific role of the LAS in the proposed pathways exist.

In particular, the role of extraframework Al (EFAL) on hydrocarbon chemistry must be considered, as this species constitutes the largest fraction of LAS in zeolites.<sup>24,25</sup> The polarization of BAS OH groups via coordinative interaction of the oxygen of the OH group with coordinatively unsaturated cations was speculated to cause higher strength of BAS in the

presence of EFAL.<sup>24,26</sup> van Bokhoven et al.<sup>27</sup> and Gounder et al.<sup>25</sup> concluded on the other hand that it was not the enhancement of the strength of Brønsted acid sites what caused the higher rates in acid catalyzed hydrocarbon reactions, but the stabilization of reactants and/or the transition states. Schallmoser et al.<sup>28</sup> showed that only EFAL in the direct vicinity of BAS caused a rate enhancement in alkane cracking via the entropic stabilization of the transition state, without lowering the activation energy. This helped finally to dismiss the earlier discussed enhancement of acid strength as the cause for the positive effect of LAS on the catalytic activity of BAS.<sup>24,26</sup>

Recently, we have observed that hydrogen transfer rates were drastically enhanced as long as methanol was present in the reactive mixture, indicating that a second hydrogen transfer pathway involving methanol was relevant under such conditions.<sup>17</sup> This second major hydrogen transfer pathway directly involves intermediates with only one carbon atom formed from methanol and generates C<sub>1-4</sub> alkanes and aromatic molecules (referred to as hydrogen transfer products in this work) at significantly higher rates than hydrogen transfer between two alkenes (Figure 1).<sup>17</sup> The formation rate of alkanes and aromatics, as estimated in Figure 1, changes with contact time and their maximum is in the range where partial conversion of MeOH is achieved (Figure 1a). Once full methanol conversion was achieved, the modest increase in HT products yield with contact time parallels the increase of HT products with a pure olefin feed.<sup>17</sup> Thus, the usually observed HT product in MTO conversion is comprised of the contribution of a methanol-induced hydrogen transfer (MIHT) in the first part of the catalytic bed and an olefin-induced HT (OIHT) pathway in the second zone of the catalyst. In particular, the MIHT rate is much higher than that of OIHT. Thus, we conclude that the formation of alkanes and aromatics in MTO is mostly associated with the MIHT pathway (Figure 1b), with only a minor contribution of the

OIHT (the evolution of ethene and propene yield on the catalyst H-ZSM-5 (B 68, L 23) is shown in Figure S.1).

In order to derive the mechanism of the hydride transfer between methanol and olefins, we explore the role of BAS and LAS in the hydride transfer routes active during methanol conversion to olefins on H-ZSM-5. The independent variation of the concentration of BAS and LAS on our H-ZSM-5 allows an unequivocal qualitative and quantitative assessment of the active sites and their importance for catalysis on a molecular level.

## 2. RESULTS AND DISCUSSION

**2.1. Role of Lewis Acid Sites on the Hydride Transfer Routes.** On the H-ZSM-5 catalysts studied (for physicochemical properties see Table 1), methanol equilibrated rapidly to

**Table 1. Studied H-ZSM-5 Samples with Corresponding Brønsted Acid Sites (BAS) and Lewis Acid Sites (LAS) Concentrations**

sample	BAS ( $\mu\text{mol/g}$ ) <sup>a</sup>	LAS ( $\mu\text{mol/g}$ ) <sup>a</sup>
H-ZSM-5 (B 113, 22)	113 $\pm$ 6	22 $\pm$ 1
H-ZSM-5 (B 68, L 39)	68 $\pm$ 3	39 $\pm$ 2
H-ZSM-5 (B 68, L 29)	68 $\pm$ 3	29 $\pm$ 1
H-ZSM-5 (B 68, L 23)	68 $\pm$ 3	23 $\pm$ 1
H-ZSM-5 (B 63, L 20)	63 $\pm$ 3	20 $\pm$ 1
H-ZSM-5 (B 71, L 66)	71 $\pm$ 4	66 $\pm$ 3
H-ZSM-5 (B 33, L 20)	33 $\pm$ 2	20 $\pm$ 1
LAS-MFI	0	14 $\pm$ 1

<sup>a</sup>Acid concentrations determined by IR spectroscopy of adsorbed pyridine.

dimethyl ether and water and was converted initially to C<sub>3</sub> and C<sub>4</sub> olefins, as well as to a small concentration of HT products (2–4 C %). Figure 2 shows the conversion and the yields of HT products (aromatics + C<sub>1–4</sub> alkanes), C<sub>3</sub><sup>=</sup> and C<sub>4</sub><sup>=</sup> olefins as a function of contact time for samples with identical BAS and varying LAS concentrations. Despite slight differences in activity at partial conversion, all catalysts reached full conversion at the same contact time (Figure 2a) regardless of the LAS concentration. Note that for every data point a fresh sample was measured and that small deviations at partial conversion typically occur in the autocatalysis reaction regime. We conclude, therefore, that the presence of LAS did not enhance the activity of BAS for methanol conversion. If LAS had a positive effect, for samples with high LAS concentration in Figure 2a, the conversion during the autocatalytic product formation (interval between W/F = 2–5 h·g<sub>cat</sub>/mol<sub>MeOH</sub>) should be higher than for samples with low concentrations, which was not observed. Thus, we conclude that the overall activity of the catalyst to convert methanol is only determined by the concentration of BAS.

The yield of aromatics and alkanes (combined as hydride transfer (HT) products in Figure 2b) decreased with decreasing LAS concentration. Note that the quantitative and qualitative increase of the corresponding olefins (Figure 2c and d) was distributed and subtle, so that it was hardly observed in a graphical representation.

Having shown that the HT ability of catalysts correlates with the LAS concentration, the question arises, whether the classic HT pathway (OIHT), the methanol induced hydride transfer (MIHT) pathway, or both are sensitive to the concentration of LAS. We have shown recently that the higher rate of hydrogen

transfer under partial conversion is caused by a large contribution of the MIHT pathway.<sup>17</sup> Because the selectivity to hydride transfer products varied in parallel with the LAS concentration over the whole conversion range (Figure 3), we conclude that lower LAS concentrations mainly decreased the contribution of the MIHT pathway.

Next, we inspect, if low concentrations of LAS affect also the OIHT pathway. For this, 1-hexene cracking was studied on H-ZSM-5 (B 68, L 39) and H-ZSM-5 (B 63, L 20). Figure 4 compiles the HT products, i.e., the sum of the yields of C<sub>1–4</sub> alkanes and aromatics, as a function of 1-hexene conversion. Over the whole conversion range, 1-hexene cracking gave rise to only minor hydrogen transfer for both catalysts. Thus, we conclude that the OIHT pathway in MTO conversion was not affected by the concentration of LAS and only depended on the BAS concentration. These results demonstrate that an increase in the LAS concentration promotes the MIHT, but does not promote hydrogen transfer between olefins and/or naphthenes as previously proposed for MTH reaction on H-ZSM-5.<sup>23</sup>

It should be noted at this point that this conclusion refers to LAS involving Al<sup>3+</sup>. Other extraframework metal cations such as La<sup>3+</sup> may polarize and activate C–H bonds in alkanes, favoring hydride and hydrogen transfer between hydrocarbons to a more significant extent.<sup>29,30</sup>

To obtain a more nuanced insight into the role of LAS for the reactions during MIHT, a catalyst with a high LAS concentration (H-ZSM-5 (B 71, L 66)) and a much higher LAS/BAS ratio than the samples shown in Figure 2 was compared with the sample H-ZSM-5 (B 68, L 23). Figure S.2 shows the changes of conversion with contact time as well as the C<sub>3</sub><sup>=</sup> and C<sub>4</sub><sup>=</sup> yields as a function of conversion. While the catalyst activity was unaffected, the C<sub>3</sub><sup>=</sup> and C<sub>4</sub><sup>=</sup> yields were slightly lower for the sample having the higher LAS concentration. Interestingly, the alkanes (Figure 5a) and aromatics (Figure 5c) yields did not vary in parallel. From ~20% conversion, the alkanes yield became higher for the catalyst with a high concentration of LAS (66  $\mu\text{mol/g}$ ), (Figure 5a). The higher yield of dienes (represented by butadiene) for H-ZSM-5 (B 71, L 66) did not occur simultaneously with that of alkanes, but only at higher conversions (>40%) (Figure 5b), indicating that alkanes and diene are formed from different reaction steps without participation of the conventional hydrogen transfer pathway (Scheme 1). Dienes are not end-products; their yield declined after 80% methanol conversion, due to further conversion to aromatics. The higher aromatics yield for H-ZSM-5 (B 71, L 66) also appeared from 40% conversion (Figure 5c). This different evolution of products with contact time, in particular the changes of alkanes and aromatics, suggests that several sequential steps are involved in MIHT. An increase in LAS concentration induces a higher alkane yield at short contact time, indicating that alkanes are a primary product of the MIHT pathway. On the other hand, a high LAS concentration favors dienes and aromatics formation with longer contact time, suggesting that they are formed from secondary reactions in MIHT.

**2.2. Role of Brønsted Acid Sites on the Hydride Transfer Routes.** In exploring the specific role of BAS for hydrogen transfer in MTO conversion, we focus in the next step on catalysts with similar low concentration of LAS (ca. 20  $\mu\text{mol/g}$ ) and varying BAS concentrations. As expected,<sup>31</sup> the initiation phase (that is, the contact time before the autocatalytic MTO conversion starts and gas phase products are detected) was shorter for catalysts with higher BAS

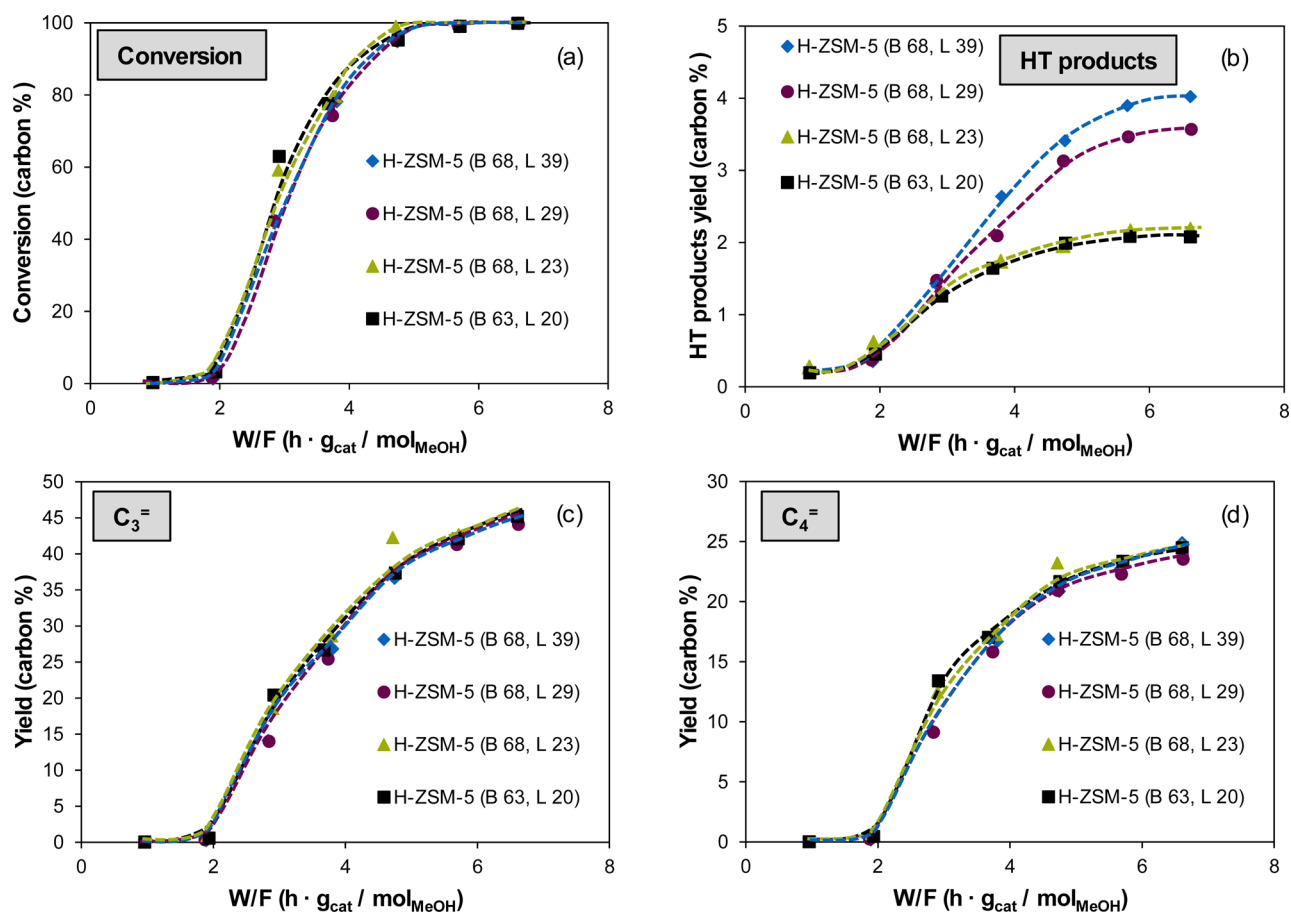


**Figure 2.** Conversion (a), yields of hydride transfer products (b), C<sub>3</sub>= olefins (c), and C<sub>4</sub>= olefins (d) as a function of contact time on H-ZSM-5 (B 68, L 39), H-ZSM-5 (B 68, L 29), H-ZSM-5 (B 68, L 23), and H-ZSM-5 (B 68, L 20) at  $p_{\text{MeOH}} = 178$  mbar and  $T = 723$  K.

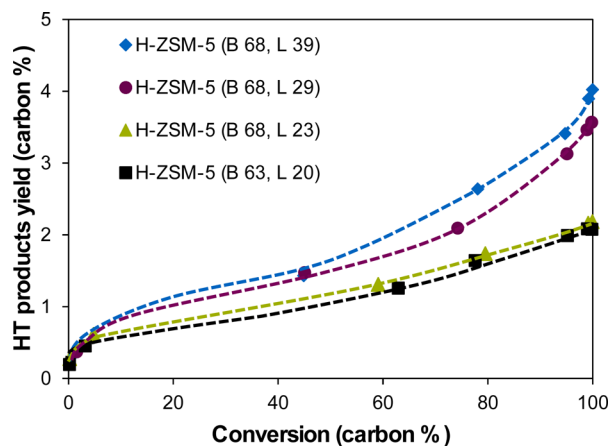


**Figure 3.** Yields of hydrogen transfer products as a function of the conversion for H-ZSM-5 samples with different LAS concentration at  $p_{\text{MeOH}} = 178$  mbar and  $T = 723$  K.

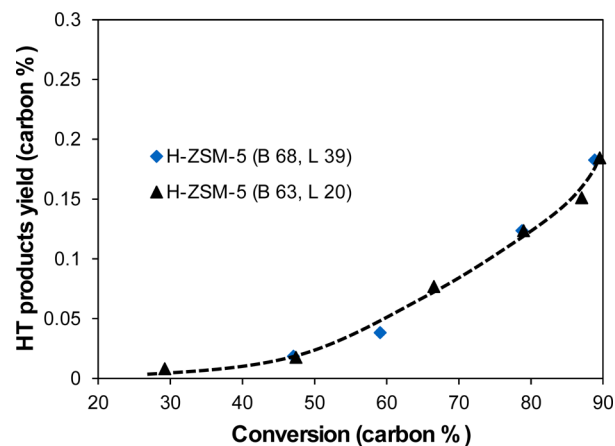


**Figure 4.** Yield of hydrogen transfer products (sum of the yields of C<sub>1-4</sub> alkanes and aromatics) as a function of 1-hexene conversion for two samples with varying LAS concentration at  $p_{1\text{-hexene}} = 29.7$  mbar and  $T = 723$  K.

concentration (Figure 6a). At the same conversion levels, less HT products were formed as the BAS concentration increased (Figure 6b). Interestingly, the selectivity difference was visible between the catalysts with BAS concentrations of 33 and 68  $\mu\text{mol/g}$ , but only marginal between the catalysts with 68 and 113  $\mu\text{mol/g}$  BAS. Thus, we conclude that the MeOH-induced hydrogen transfer, having a remarkably higher rate at partial methanol conversion (Figure 1, ref 17), was hardly affected by the increase of BAS concentration between 68 to 113  $\mu\text{mol/g}$ .

Noticeably, an additional increase of HT products was observed at total methanol conversion for H-ZSM-5 (B 113, L 22). This is attributed to the substantial propagation of OIHT at high BAS concentration. To prove this hypothesis, 1-hexene cracking experiments were conducted on the catalysts H-ZSM-5 (B 113, L 22) and H-ZSM-5 (B 68, L 23). A higher conversion rate was obtained by increasing the BAS concentration (Figure S.3). The selectivity to HT products is

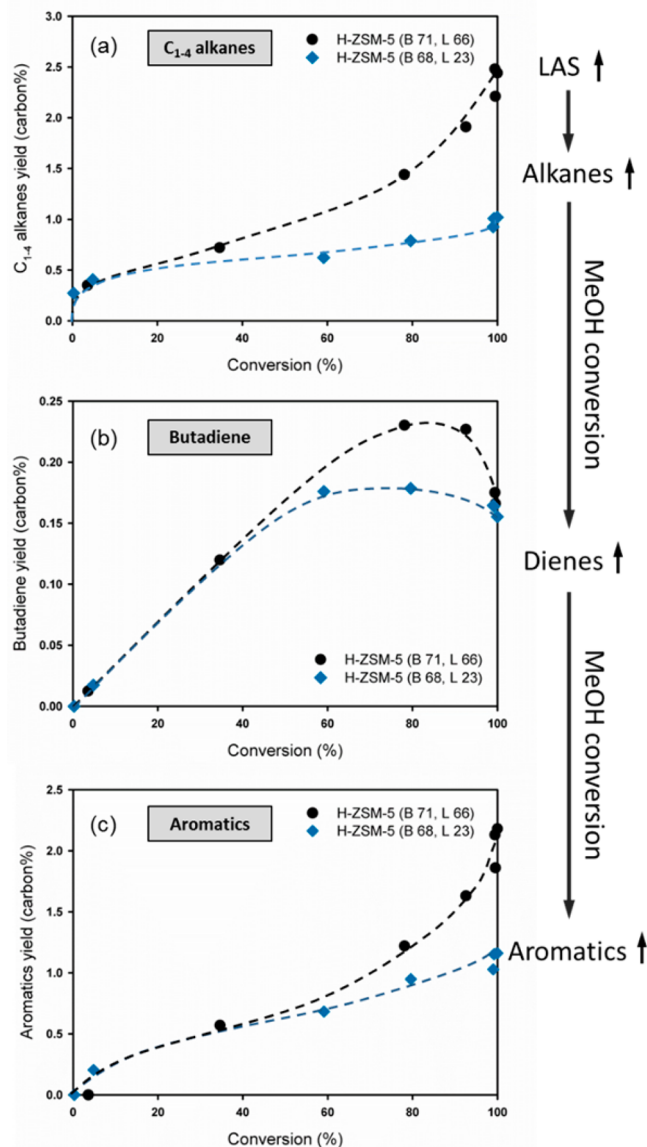


**Figure 5.** Alkanes (a), butadienes (b), and aromatics (c) yield as a function of methanol conversion on H-ZSM-5 (B 68, L 23) and H-ZSM-5 (B 71, L 66) at  $p_{\text{MeOH}} = 178$  mbar and  $T = 723$  K.

shown by their yield versus 1-hexene conversion in Figure 7. It is evident that the yield of HT products varied with conversion in identical manner, showing that the changes observed in Figure 6b in the full conversion range were caused only by the longer contact time of olefins with the BAS active sites. In other words, for contact times beyond full methanol conversion, the contribution of OIHT to the HT yield of MTO becomes relevant and the effect is stronger for those catalysts with a relative high concentration of BAS sites. At partial conversions, the presence of methanol inhibits olefin adsorption at BAS even at low concentrations,<sup>32</sup> making this route negligibly small. Thus, we conclude that a majority of the hydrogen transfer products in MTO are formed by MIHT (involving LAS and BAS) at partial conversion and that the contribution of the olefin-induced HT (involving only BAS) is only relevant in the section of catalyst bed operating after full methanol conversion has been reached.

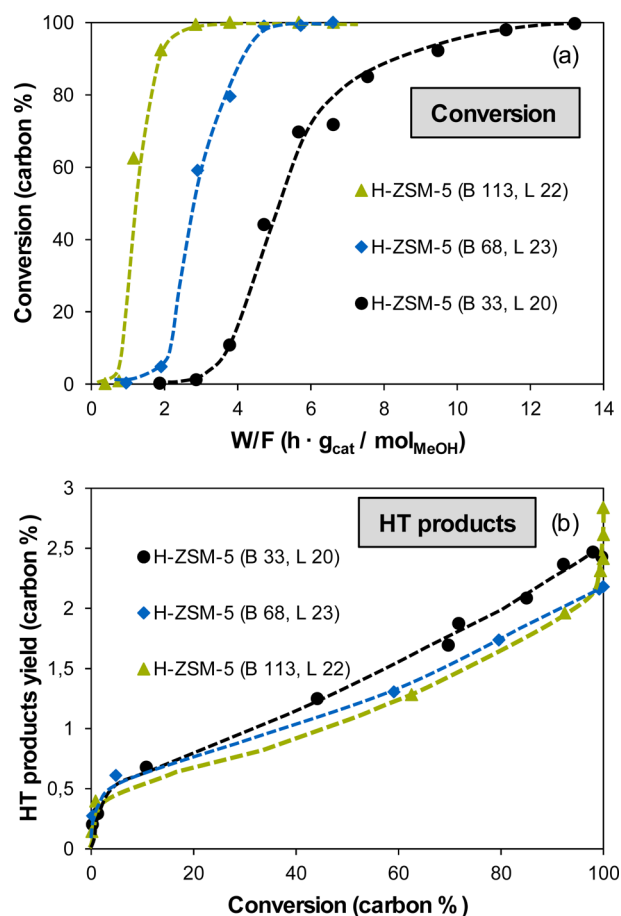


**Figure 6.** Change of conversion with contact time (a) and change of HT products yield with conversion (b) at  $p_{\text{MeOH}} = 178$  mbar and  $T = 723$  K.

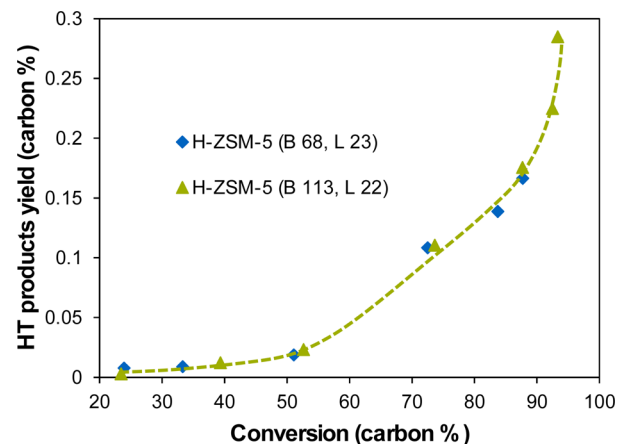


**Figure 7.** Change of HT products yield with 1-hexene conversion for two samples with different BAS concentration at  $p_{1\text{-hexene}} = 29.7$  mbar and  $T = 723$  K.

Selectivity to HT products (at contact times when full methanol conversion has just been reached) is shown in Figure 8 in regard of BAS and LAS concentrations. The contact time was selected so that methanol and dimethyl ether conversion reached a value of almost 100% conversion. Thus, it is hypothesized that HT products at the contact time mostly form via the MIHT pathway. Figure 8 shows that the HT products selectivity increased linearly with LAS concentration for

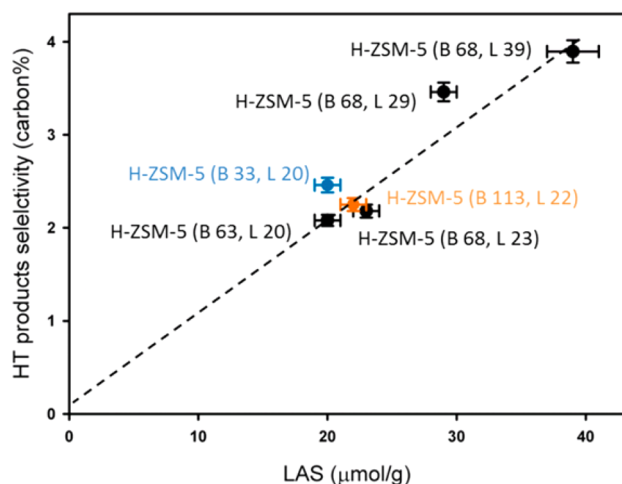


**Figure 8.** Correlation of HT products selectivity with LAS concentration for H-ZSM-5 samples, when just reaching complete MeOH conversion.  $T = 723$  K,  $p_{\text{MeOH}} = 178$  mbar, contact time 2.8 h· $g_{\text{cat}}/\text{mol}_{\text{MeOH}}$  for H-ZSM-5 (B113, L22) and 13.2 h· $g_{\text{cat}}/\text{mol}_{\text{MeOH}}$  for H-ZSM-5 (B33, L20); contact time 6.6 h· $g_{\text{cat}}/\text{mol}_{\text{MeOH}}$  for all other samples.

samples with same BAS concentration. Conversely, BAS concentration has very limited impact on HT products selectivity, where an increase of BAS from 33  $\mu\text{mol/g}$  to 113  $\mu\text{mol/g}$  merely led to a difference of 0.3 C % of the HT yield. An extrapolation of the line would intercept the axes close to the origin, which also supports that hydrogen transfer on solely BAS in the absence of LAS is very slow. Thus, LAS are indispensable for MIHT.

**2.3. Mechanism of the MeOH-Induced Hydrogen Transfer Pathway.** We have shown that both BAS and LAS are involved in MIHT and that LAS are indispensable active sites for the MIHT to occur. Recently, we had reported HCHO to form during MTO by hydrogen transfer<sup>17,33</sup> and to be involved in the formation of O-containing coke species.<sup>17,34</sup> Thus, we hypothesize that the MIHT is a reaction between methanol and alkenes catalyzed by LAS of H-ZSM-5, yielding HCHO and alkanes as products. The formed HCHO readily reacts with hydrocarbons and hence cannot be detected in the gas phase MTO outlet.

In order to test the participation of HCHO as a reaction intermediate, we used transient experiments with 1-methoxypropane ( $\text{CH}_3\text{OC}_3\text{H}_7$ ), which decomposes under reaction conditions into methanol/dimethyl ether and propene. This allows monitoring the surface reaction of methanol with an olefin at very low partial pressures, so avoiding secondary reactions. The role of LAS catalyzed reactions was then tested using a ZSM-5 sample containing only LAS (LAS-MFI), prepared by reacting  $\text{Al}(\text{OC}_2\text{H}_5)_3$  with the defect sites of silicalite. The gas phase products analyzed by IR spectroscopy (Figure 9, middle) after admitting a pulse of 1-methoxypropane shows clearly the formation of propene and methanol. After 30 s, HCHO was detected (Figure 9, top), suggesting that HCHO was strongly adsorbed on LAS-MFI.

Thus, we infer that propene acts as hydrogen acceptor, forming stoichiometric amounts of propene. Note that overlapping bands in the C–H region did not allow a quantitative assessment. Continuous reaction on LAS-MFI at 623 K in a plug-flow reactor ( $p_{1\text{-methoxypropane}} = 178$  mbar,  $W/F = 0.35$  h· $g_{\text{cat}}/\text{mol}_{1\text{-methoxypropane}}$ ) led to propene and methanol/

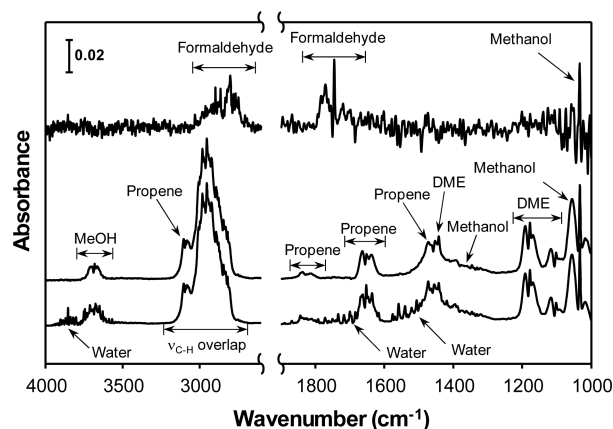


**Figure 9.** IR spectra of gas phase products after pulsing 0.5  $\mu\text{L}$  of 1-methoxypropane over pure LAS-MFI at 723 K: IR spectrum collected 10 s after injection (bottom), IR spectrum collected 10 s after injection with subtracted gas phase water (middle) and IR spectrum collected 30 s after injection with subtracted gas phase water (intensity  $\times 100$ ; top). The band assignment is according to the IR spectra of water, propene, MeOH, DME and formaldehyde shown in the database NIST Chemistry WebBook (<http://webbook.nist.gov/chemistry/>).

dimethyl ether as well as propane in the gas phase (Table S.1). The FID response of HCHO is very low,<sup>35</sup> limiting the detectability of HCHO. Combining both results, we conclude that extra lattice alumina (LAS) catalyzes the hydrogen transfer between methanol and light olefins to form HCHO and alkanes.

Having shown that HCHO is readily generated at LAS, the impact of HCHO on H-ZSM-5 (B 68, L 39) was explored using dimethoxymethane (DMM). Under reaction conditions, DMM hydrolyzes into methanol and formaldehyde with stoichiometry of 2/1.<sup>36</sup> Thus, cofeeding 3 C % dimethoxymethane to methanol is regarded as equivalent to cofeeding ca. 1 C % HCHO.

Figure S.4 shows the conversion of the pure methanol feed and of the feed containing HCHO (1 C %) on H-ZSM-5 (B 68, L 39) as a function of contact time. Over the whole range of contact time, the conversion was slightly lower when cofeeding HCHO. Formaldehyde also reduced slightly the selectivity toward propene and butenes (Figure S.5) at conversions above 60 C %. In contrast, the aromatics yield was higher at all conversions (Figure 10a). Interestingly, the overall alkanes yield (Figure 10b) was unaffected by HCHO cofeeding. If alkanes were produced via the OIHT pathway, alkanes and aromatic molecules should vary in parallel.<sup>4</sup> Thus, the variation in the yield of aromatic molecules without affecting the yield of alkanes provides the first evidence of two pathways, one in which alkanes are formed together with HCHO and a second pathway producing aromatic molecules from formaldehyde and alkenes. In particular, the formation of aromatics from the second pathway does not require an olefin as H-acceptor and consequently no alkane is formed in this pathway, if HCHO is supplied directly (not formed from methanol).

Thus, overall we conclude that high concentrations of LAS induce the formation of HCHO and a higher yield of alkanes. Subsequently, HCHO induces the formation of aromatic molecules as deduced from the deviations in the yields for alkanes and aromatic molecules.

After showing how LAS and BAS catalyze the MIHT route with HCHO as the linking intermediate, we address next the

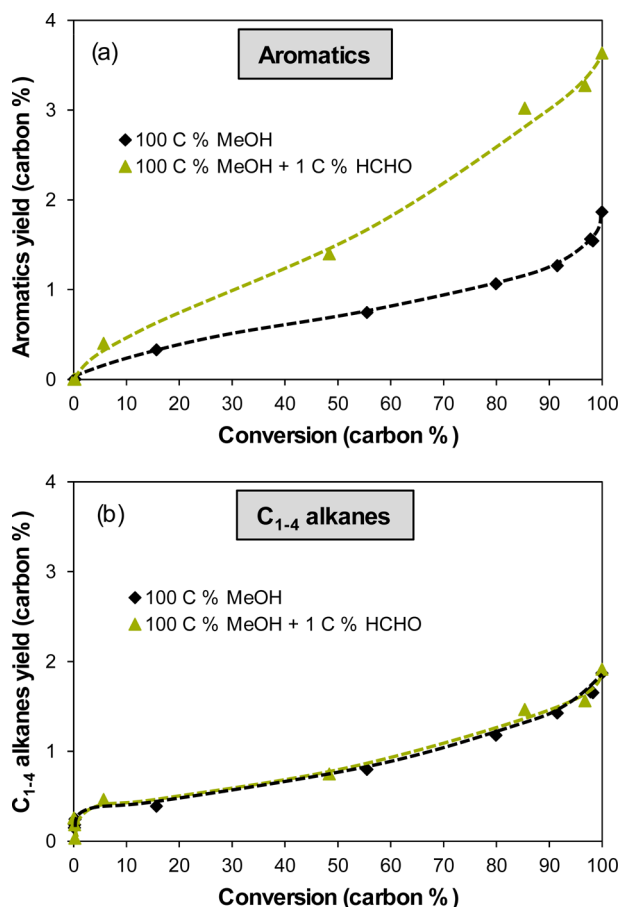


**Figure 10.** Change of aromatics (a) and C<sub>1-4</sub> alkanes (b) yield with conversion for the pure MeOH feed and the feed containing 1 C % HCHO on H-ZSM-5 (B 68, L 39) at  $p_{\text{MeOH}} = 100$  mbar and  $T = 723$  K.

active acid sites for the further conversion of HCHO. Experiments with HCHO (DMM) cofeeding showed a slower reaction rate of methanol in MTO (Figure S.4). This suggests that HCHO chemisorbs on BAS more strongly than MeOH, hindering the conversion of MeOH through the olefin cycle. Therefore, when BAS/LAS ratios are low, the formation of aromatics from HCHO competes with independent reactions of methanol. To rule out LAS catalyzed aldol condensation involving HCHO,<sup>37</sup> cofeeding experiments were carried out with two catalysts with nearly identical BAS and differing LAS concentration (H-ZSM-5 (B 63, L 20) and H-ZSM-5 (B 68, L 39)). Both catalysts had similar activity in MTO (Figure S.6), allowing a direct comparison of the aromatics and C<sub>1-4</sub> alkanes yields (Figure S.7).

Both alkanes and aromatic yields obtained on H-ZSM-5 (B 63, L 39) were higher than the corresponding yields obtained on H-ZSM-5 (B 68, L 20). The increase in alkanes yield on H-ZSM-5 (B 63, L 39) is attributed to hydride transfer from methanol on LAS and is unaffected by the concentration of HCHO. The aromatics yield was only slightly higher (0.7 C %) with the higher concentration of LAS than that for a lower LAS concentration, and even lower than the 1 C % increase observed in alkanes yield. If the aromatic molecules were formed by a reaction of HCHO and olefins on LAS, cofeeding HCHO should have led to higher yields with the H-ZSM-5 having the higher LAS concentration. The higher LAS concentration should have led to the formation of more

HCHO (from methanol), which together with the HCHO additionally co-fed should result in a higher aromatics yield. Therefore, it is concluded that the aromatics formation involving HCHO is catalyzed only by BAS.

This conclusion is supported by the results of coprocessing HCHO with methanol on H-ZSM-5 with different BAS concentrations and nearly identical LAS concentrations. Due to differences in catalyst activity (Figure S.8), the aromatics yield is illustrated as a function of conversion (Figure 11).

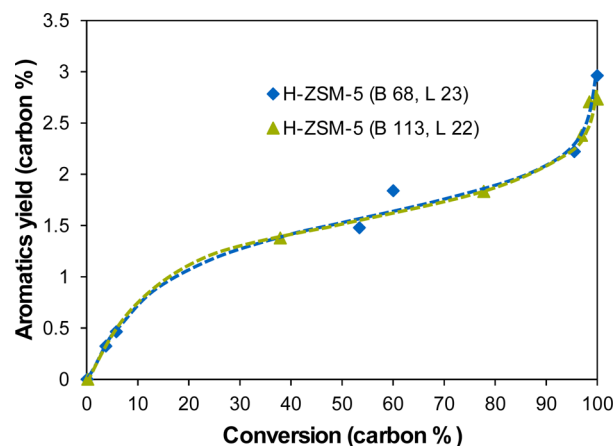


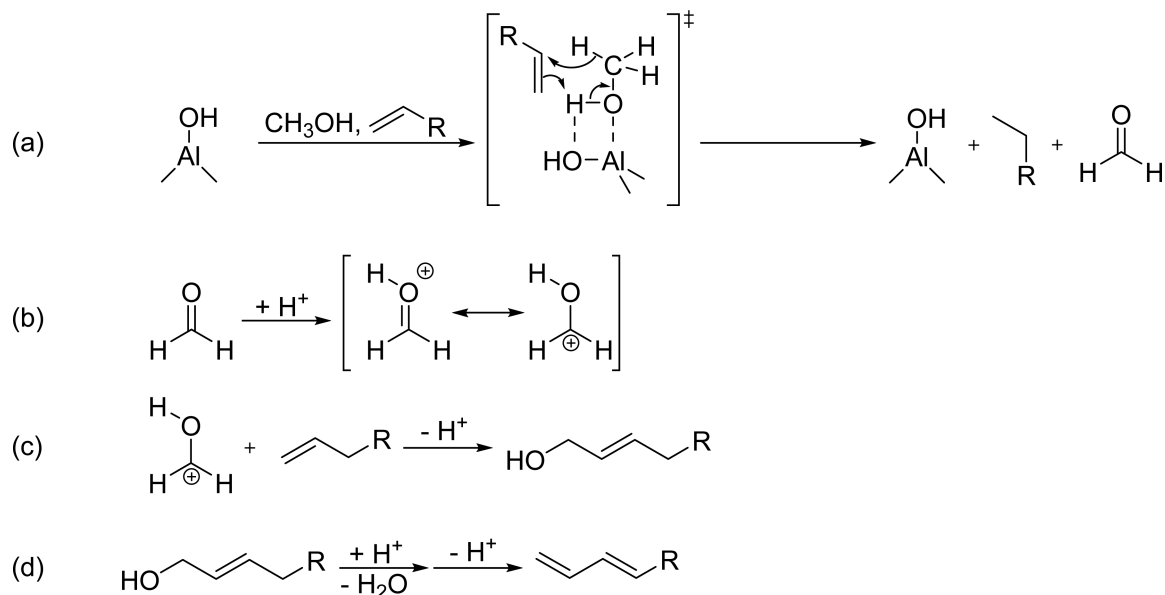
**Figure 11.** Aromatics yield as a function of conversion for a feed of methanol with 1 C % HCHO over H-ZSM-5 (B 68, L 23) and H-ZSM-5 (B 113, L 22) at  $p_{\text{MeOH}} = 100$  mbar at  $T = 723$  K.

Addition of HCHO enhanced the selectivity to aromatic molecules in a similar extent for samples with the same LAS concentration, even if their BAS concentration varied significantly. From this result, it is inferred that HCHO – either co-fed or generated over LAS – chemisorbs on BAS more strongly than methanol and hydrocarbons. We hypothesize that the formation of aromatics via HCHO involvement at a given HCHO concentration only depends on the partial pressure of the other reactant (alkenes) in the mobile phase. The concentration of alkenes in the mobile phase is determined by the overall MTO conversion and, thus, by the concentration of BAS. For this reason, differences in the selectivity to aromatics were not observed when HCHO was co-fed on catalysts with same LAS, but different BAS concentration (Figure 11).

**2.4. Routes to the Formation of Alkanes and Aromatic Molecules.** In the first step of the MIHT route, alkanes are generated at LAS. Hydrogen from methanol is transferred to an alkene, generating HCHO and an alkane.

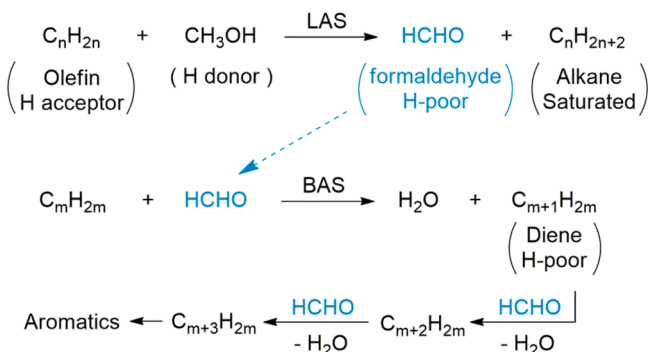
For MeOH activation on LAS, it is proposed that MeOH coordinatively interacts with the LAS (Scheme 3a), whereby the O–H bond is weakened. Adsorbed methanol may react with olefins in a concerted mechanism via a six-membered transition state to alkanes and HCHO.

The reaction of LAS-generated HCHO on BAS with alkenes would then lead to dienes, higher unsaturated olefins and, ultimately, aromatics. In such a pathway, HCHO is protonated at BAS (Scheme 3b) and then reacts with olefins in a nucleophilic addition to an allylic alcohol (Scheme 3c). Dehydration of this allylic alcohol leads to the formation of a diene (Scheme 3d). The diene species reacts further with a second HCHO, and is converted to a more H-poor molecule with higher degree of unsaturation (Scheme 4). The

Scheme 3. Proposed Individual Reactions for the Formation of Dienes and Alkanes in the MeOH-Mediated Pathway<sup>a</sup>

<sup>a</sup>LAS are schematically represented by Al–OH end groups.

Scheme 4. Schematic Reaction Network for Methanol-Mediated Alkanes and Aromatics Formation Involving Alkanes from Methanol-Induced Hydrogen Transfer at Lewis Acid Sites and Aromatics from Formaldehyde Based Reactions at Brønsted Acid Sites



propagation of such reactions with HCHO will increase the length of the carbon chains and accumulate the degree of unsaturation, ultimately forming aromatics (Scheme 4). The stepwise additions of adsorbed HCHO to olefins are Brønsted acid catalyzed. The formation of aromatic molecules in the MIHT pathway requires, thus, both LAS and BAS. However, mostly zeolites contain abundant amount of BAS than LAS, which makes the reaction on LAS as the overall rate-determining step for aromatics formation. Only on the zeolite with a low BAS/LAS ratio, i.e., H-ZSM-5 (B 71, L66), the reactions catalyzed by BAS would limit the formation of dienes and aromatics so that we could observe them as secondary products.

### 3. CONCLUSION

Two hydride transfer routes were identified for the conversion of methanol to hydrocarbons. One requires the presence of methanol and involves the formation of HCHO transferring the hydrogen to alkenes. The other operates in the absence of methanol, transferring hydrogen between alkenes. Hydrogen

transfer in the presence of methanol is promoted with increasing LAS concentration, showing quantitatively that LAS are involved in the rate-determining step. In the absence of methanol, the concentration of LAS did not affect the rate of formation of HT products under identical reaction conditions, even for a reactant stream containing only alkenes. The rate of this HT reaction in the absence of methanol was solely related to the concentration of BAS. Thus, the present experiments show unequivocally that methanol is involved in a hydride transfer route, which is catalyzed by LAS. This MeOH-induced hydrogen transfer route was identified to be the dominant pathway to aromatic molecules as well as light alkanes. The pathway consists of two individual steps, which are catalyzed by LAS and BAS and are linked by HCHO as an intermediate product. Formaldehyde is formed by transferring two H atoms in MeOH to an alkene on a LAS. Then another alkene reacts stepwise with several HCHO at BAS to form dienes and ultimately aromatics.

The qualitative and quantitative understanding of these elementary processes is the key to design better and more stable catalysts for the conversion of methanol to hydrocarbons, and gives a clear blueprint for material synthesis of new catalysts.

## 4. EXPERIMENTAL SECTION

**4.1. Zeolite Samples and Chemicals.** The H-ZSM-5 samples used in this study (Table 1) were provided by Clariant Produkte (Deutschland) GmbH and are denoted as H-ZSM-5 (B X, L Y), where “B X” and “L Y” stand for the BAS and LAS concentration in  $\mu\text{mol/g}$  of the catalysts, respectively. The powder pattern of sample H-ZSM-5 (B 68, L 39) is shown in Figure S.9. No differences in XRD patterns were observed for the other H-ZSM-5 samples reported in this contribution.

The LAS-MFI catalyst was prepared by treating a silicalite sample with  $\text{Al}(\text{OC}_2\text{H}_5)_3$ . A controlled amount of  $\text{Al}(\text{OC}_2\text{H}_5)_3$  and silicalite was dispersed in 50 mL solvent containing 25 mL of methanol and ethanol. The slurry was transferred to a pressure glass tube and sealed. The tube was placed in an oil bath (373 K) and kept for 5 h under agitation. Subsequently, the solvent was removed by evacuation. The solid was washed with hot ethanol for one time and hot water for two



times. Subsequently, it was dried at 373 K overnight and calcined in flowing synthetic air (100 mL/min) at 823 K for 4 h. After cooling, the powder was stored in a bottle and ready for use.

Methanol ( $\geq 99.9\%$ ),  $\text{Al}(\text{OC}_2\text{H}_5)_3$  (97%), and ethanol (99.8%) were supplied by Sigma-Aldrich.

**4.2. Characterization of Acid Sites.** IR spectroscopy was used to determine the acid site concentrations of zeolites by pyridine (purity 99.8%, Sigma-Aldrich) adsorption. All spectra were collected at 423 K on a Nicolet 5700 FT-IR spectrometer. Zeolite samples were pressed into wafers and pretreated in vacuum ( $<10^{-5}$  mbar) at 723 K for 1 h. Then they were exposed to 0.1 mbar pyridine at 423 K for 0.5 h. Physisorbed pyridine was removed by 1 h evacuation at 423 K; pyridine adsorbed on weak acid sites was removed by outgassing at 723 K for 0.5 h. The concentration of Brønsted and Lewis acid sites was quantified based on the band area at  $1515\text{--}1565\text{ cm}^{-1}$  and  $1435\text{--}1470\text{ cm}^{-1}$  normalized to the wafer weight. Molar absorption coefficients used were  $\epsilon$  (BAS) =  $1.67\text{ cm}^2/\mu\text{mol}$  and  $\epsilon$  (LAS) =  $2.22\text{ cm}^2/\mu\text{mol}$ .

**4.3. Catalytic Testing.** All catalytic tests were conducted in tubular flow reactors with an internal diameter of 6 mm of the quartz tube at ambient pressure. The catalyst powders were pelletized, crushed, and used in a sieve fraction ranging from 200 to 280  $\mu\text{m}$ . For the reactions, the catalyst pellets were homogeneously diluted with silicon carbide (ESK-SiC) in the range of 355–500  $\mu\text{m}$  to ensure temperature uniformity. The samples were activated at 723 K with 50 mL/min  $\text{N}_2$  for 1 h.

In order to evaluate the performance of catalysts in the MTO conversion, 50 mL/min  $\text{N}_2$  was passed through the methanol (purity  $\geq 99.9\%$ , Sigma-Aldrich) saturator with the temperature controlled at 299 K resulting in a MeOH partial pressure of 178 mbar. The reaction was typically conducted at 723 K. Weight hourly space times were adjusted by varying the catalyst loading.

In the HCHO cofeeding experiments, the methanol partial pressure was maintained at 100 mbar. Methanol was fed by passing dry  $\text{N}_2$  flow through a methanol evaporator kept at 299 K. HCHO was generated by introducing dimethoxymethane (DMM) (purity 99%, Sigma-Aldrich) which hydrolyzes into methanol/dimethyl ether and HCHO, producing approximately 1 mol of HCHO per mol of DMM converted.<sup>36</sup> The co-fed DMM vapor was adjusted by flowing  $\text{N}_2$  through a saturator containing the liquid reactant at a temperature of 273 K. Catalyst loading and reactant flow velocity were varied to achieve a wide range of contact time and methanol conversion. For these experiments, the contact time was defined as the ratio of catalyst mass to the molar flow rate of methanol.

To investigate the role of olefin-induced HT in methanol conversion, experiments were conducted at similar reaction conditions, but with pure olefin feed. Dry  $\text{N}_2$  was passed through a 1-hexene (purity  $\geq 99\%$ , Sigma-Aldrich) saturator kept at 283 K and subsequently diluted with  $\text{N}_2$ , so that experiments at a 1-hexene partial pressure of 29.7 mbar were conducted.

For the conversion of 1-methoxypropane ( $\text{CH}_3\text{OC}_3\text{H}_7$ ) (purity 97%, Sigma-Aldrich) on LAS-MFI at 623 K, dry  $\text{N}_2$  was passed through a  $\text{CH}_3\text{OC}_3\text{H}_7$  saturator kept at 273 K. By further  $\text{N}_2$  dilution a partial pressure of 178 mbar was obtained.

The reactor effluents were analyzed by a HP 5890 gas chromatograph equipped with a HP-PLOTQ capillary column (30 m, 0.32 mm inner diameter) and a flame ionization detector for online analysis.

Due to their fast interconversion, both methanol and dimethyl ether were treated as reactants. Conversion and yields were calculated on a carbon basis. The  $\text{C}_5$  fraction designates all hydrocarbons with five carbon atoms and the  $\text{C}_{6+}$  aliphatics fraction includes all other heavier hydrocarbons other than aromatics.

Rates are calculated as site time yield, the yield increase within a certain contact time:  $r = \frac{d(\text{yield})}{d(\text{contact time})}$ .

**4.4. Pulse Reaction with 1-Methoxypropane ( $\text{CH}_3\text{OC}_3\text{H}_7$ ) on LAS-MFI.** Pulse reactions were carried out on a LAS-MFI (Al-modified silicalite) catalyst in the same reactor tube as used for the experiments in subsection 4.3 at 723 K under 25 mL/min He flow, but connected to a homemade IR cell to detect gas phase products. Each

time, 0.5  $\mu\text{L}$   $\text{CH}_3\text{OC}_3\text{H}_7$  was injected into the flow and IR spectra were collected every 10 s after injection.

## ■ ASSOCIATED CONTENT

### 📄 Supporting Information

The Supporting Information is available free of charge on the ACS Publications website at DOI: 10.1021/jacs.6b09605.

Additional results on the conversion and product distribution for MeOH reaction, MeOH/DMM cofeeding reaction, 1-hexene reaction and 1-methoxypropane reaction; XRD pattern of the sample H-ZSM-5 (B 68, L 39) (PDF)

## ■ AUTHOR INFORMATION

### Corresponding Authors

\*m.sanchez@tum.de

\*johannes.lercher@ch.tum.de

### ORCID

Felix M. Kirchberger: 0000-0001-6321-6456

Johannes A. Lercher: 0000-0002-2495-1404

### Present Address

<sup>†</sup>S.M.: Paul Scherrer Institute, Bioenergy and Catalysis Laboratory, 5232 Villigen PSI, Switzerland.

### Author Contributions

<sup>§</sup>S.M. and Y.L. contributed equally to this work.

### Notes

The authors declare no competing financial interest.

## ■ ACKNOWLEDGMENTS

The financial support from Clariant Produkte (Deutschland) GmbH and fruitful discussions within the framework of MuniCat are gratefully acknowledged. S.M. is thankful to Elisabeth Hanrieder for helpful discussions.

## ■ REFERENCES

- (1) Olsbye, U.; Svelle, S.; Bjørgen, M.; Beato, P.; Janssens, T. V. W.; Joensen, F.; Bordiga, S.; Lillerud, K. P. *Angew. Chem., Int. Ed.* **2012**, *51*, 5810–5831.
- (2) Ilias, S.; Bhan, A. *ACS Catal.* **2013**, *3*, 18–31.
- (3) Stöcker, M. *Microporous Mesoporous Mater.* **1999**, *29*, 3–48.
- (4) Sun, X.; Mueller, S.; Shi, H.; Haller, G. L.; Sanchez-Sanchez, M.; van Veen, A. C.; Lercher, J. A. *J. Catal.* **2014**, *314*, 21–31.
- (5) Kazansky, V. B.; Frash, M. V.; van Santen, R. A. Quantum-chemical study of hydride transfer in catalytic transformation of paraffins on zeolites. In *Studies in Surface Science and Catalysis*; Chon, H., Ihm, S.-K., Uh, Y. S., Eds.; Elsevier: Amsterdam, 1997; Vol. 105, pp 2283–2290.
- (6) Kazansky, V. B.; Frash, M. V.; van Santen, R. A. *Catal. Lett.* **1997**, *48*, 61–67.
- (7) Boronat, M.; Viruela, P.; Corma, A. *J. Phys. Chem. B* **1999**, *103*, 7809–7821.
- (8) Boronat, M.; Viruela, P.; Corma, A. *Phys. Chem. Chem. Phys.* **2000**, *2*, 3327–3333.
- (9) Ilias, S.; Bhan, A. *J. Catal.* **2012**, *290*, 186–192.
- (10) Simonetti, D. A.; Ahn, J. H.; Iglesia, E. *J. Catal.* **2011**, *277*, 173–195.
- (11) Simonetti, D. A.; Ahn, J. H.; Iglesia, E. *ChemCatChem* **2011**, *3*, 704–718.
- (12) Bercaw, J. E.; Diaconescu, P. L.; Grubbs, R. H.; Kay, R. D.; Kitching, S.; Labinger, J. A.; Li, X.; Mehrkhodavandi, P.; Morris, G. E.; Sunley, G. J.; Vagner, P. *J. Org. Chem.* **2006**, *71*, 8907–8917.
- (13) Bercaw, J. E.; Diaconescu, P. L.; Grubbs, R. H.; Hazari, N.; Kay, R. D.; Labinger, J. A.; Mehrkhodavandi, P.; Morris, G. E.; Sunley, G. J.; Vagner, P. *Inorg. Chem.* **2007**, *46*, 11371–11380.

- (14) Bercaw, J. E.; Grubbs, R. H.; Hazari, N.; Labinger, J. A.; Li, X. *Chem. Commun.* **2007**, 2974–2976.
- (15) Bercaw, J. E.; Hazari, N.; Labinger, J. A.; Scott, V. J.; Sunley, G. *J. J. Am. Chem. Soc.* **2008**, *130*, 11988–11995.
- (16) Hazari, N.; Labinger, J. A.; Scott, V. J. *J. Catal.* **2009**, *263*, 266–276.
- (17) Sun, X.; Mueller, S.; Liu, Y.; Shi, H.; Haller, G. L.; Sanchez-Sanchez, M.; van Veen, A. C.; Lercher, J. A. *J. Catal.* **2014**, *317*, 185–197.
- (18) Bjørgen, M.; Svelle, S.; Joensen, F.; Nerlov, J.; Kolboe, S.; Bonino, F.; Palumbo, L.; Bordiga, S.; Olsbye, U. *J. Catal.* **2007**, *249*, 195–207.
- (19) Lukyanov, D. B. *J. Catal.* **1994**, *147*, 494–499.
- (20) Bortnovsky, O.; Sazama, P.; Wichterlova, B. *Appl. Catal., A* **2005**, *287*, 203–213.
- (21) Wichterlová, B.; Žilková, N.; Uvarova, E.; Čejka, J.; Sarv, P.; Paganini, C.; Lercher, J. A. *Appl. Catal., A* **1999**, *182*, 297–308.
- (22) Čejka, J.; Žilková, N.; Tvarůžková, Z.; Wichterlová, B. Contribution of framework and extraframework Al and Fe cations in ZSM-5 to disproportionation and C<sub>3</sub> alkylation of toluene. In *Studies in Surface Science and Catalysis*; Laurent, B., Serge, K., Eds.; Elsevier: Amsterdam, 1995; Vol. 97, pp 401–408.
- (23) Sazama, P.; Wichterlova, B.; Dedeczek, J.; Tvaruzkova, Z.; Musilova, Z.; Palumbo, L.; Sklenak, S.; Gonsiorova, O. *Microporous Mesoporous Mater.* **2011**, *143*, 87–96.
- (24) Li, S.; Zheng, A.; Su, Y.; Zhang, H.; Chen, L.; Yang, J.; Ye, C.; Deng, F. *J. Am. Chem. Soc.* **2007**, *129*, 11161–11171.
- (25) Gounder, R.; Jones, A. J.; Carr, R. T.; Iglesia, E. *J. Catal.* **2012**, *286*, 214–223.
- (26) Mirodatos, C.; Barthomeuf, D. *J. Chem. Soc., Chem. Commun.* **1981**, 39–40.
- (27) van Bokhoven, J. A.; Tromp, M.; Koningsberger, D. C.; Miller, J. T.; Pieterse, J. A. Z.; Lercher, J. A.; Williams, B. A.; Kung, H. H. *J. Catal.* **2001**, *202*, 129–140.
- (28) Schallmoser, S.; Ikuno, T.; Wagenhofer, M. F.; Kolvenbach, R.; Haller, G. L.; Sanchez-Sanchez, M.; Lercher, J. A. *J. Catal.* **2014**, *316*, 93–102.
- (29) Schüßler, F.; Schallmoser, S.; Shi, H.; Haller, G. L.; Ember, E.; Lercher, J. A. *ACS Catal.* **2014**, *4*, 1743–1752.
- (30) Sievers, C.; Onda, A.; Olindo, R.; Lercher, J. A. *J. Phys. Chem. C* **2007**, *111*, 5454–5464.
- (31) Chen, J.; Li, J.; Yuan, C.; Xu, S.; Wei, Y.; Wang, Q.; Zhou, Y.; Wang, J.; Zhang, M.; He, Y.; Xu, S.; Liu, Z. *Catal. Sci. Technol.* **2014**, *4*, 3268–3277.
- (32) Wu, W.; Guo, W.; Xiao, W.; Luo, M. *Chem. Eng. Sci.* **2011**, *66*, 4722–4732.
- (33) Liu, Y.; Müller, S.; Berger, D.; Jelic, J.; Reuter, K.; Tonigold, M.; Sanchez-Sanchez, M.; Lercher, J. A. *Angew. Chem., Int. Ed.* **2016**, *55*, 5723–5726.
- (34) Müller, S.; Liu, Y.; Vishnuvarthan, M.; Sun, X.; van Veen, A. C.; Haller, G. L.; Sanchez-Sanchez, M.; Lercher, J. A. *J. Catal.* **2015**, *325*, 48–59.
- (35) Dojahn, J. G.; Wentworth, W. E.; Stearns, S. D. *J. Chromatogr. Sci.* **2001**, *39*, 54–58.
- (36) Pechenkin, A. A.; Badmaev, S. D.; Belyaev, V. D.; Sobyenin, V. A. *Appl. Catal., B* **2015**, *166–167*, 535–543.
- (37) Dumitriu, E.; Hulea, V.; Fechet, I.; Auroux, A.; Lacaze, J.-F.; Guimon, C. *Microporous Mesoporous Mater.* **2001**, *43*, 341–359.